

# Optimization of Diffusion-Controlled Free Radical Polymerizations in Lumped-Parameter Systems

Y. J. HUANG and L. JAMES LEE,\* *Department of Chemical Engineering, The Ohio State University, Columbus, Ohio 43210*

## Synopsis

Open-loop optimal temperature control strategies for the batch free radical polymerizations of styrene are investigated using the minimum principle. Two kinetic models, one considering the gel effect and the other incorporating both the gel effect and the glass effect, are employed. By using the Min-H strategy, a control variable program that minimizes one objective function and yields values of other terminal quantities can be obtained. It is found that the optimal temperature programs are highly dependent upon the kinetic characteristics of reactions. The gel and glass effects, which control ultimate molecular weights, play important roles in affecting the temperature programs. Numerical examples using two objective functions, one in which reaction time is minimized, and the other in which molecular weight distribution is minimized, are presented. The theoretical predictions using kinetic model with the gel and glass effects are also compared with experimental measurements of conversion, molecular weight, and molecular weight distribution. Although the agreement between the experimental work and the theory is less than satisfactory, the trends of policy improvements are consistent.

## INTRODUCTION

Many polymers are produced in homogeneous reaction media; the free radical bulk polymerization of styrene and methyl methacrylate (MMA), the condensation polymerization of polyesters and nylons, and the ionic polymerizations of butadiene and styrene, to mention a few. The optimization of these polymerization processes has long been of interest to researchers. A comprehensive review concerning optimization and control of polymerization reactors, including mathematical models and on-line sensors, has been conducted by MacGregor et al.<sup>1</sup>

Optimal temperature or initiator addition policies that minimize reaction times<sup>2-8</sup> or the breadth of the molecular weight distribution<sup>9-11</sup> for chain addition polymerization in homogeneous batch reactors, known as lumped-parameter systems, have been investigated quite extensively. For optimization of copolymerization reactors, Chen and co-workers<sup>12,13</sup> have studied minimum end time policies for batchwise radical chain polymerization using the initiator feed rate and temperature as two control variables. Tsoukas et al.<sup>14</sup> and Farber<sup>15</sup> have investigated multiobjective optimization problems having dual objectives of narrowing both copolymer composition and molecular weight distributions. The optimization of condensation polymerizations of nylon 6 and poly(ethylene terephthalate) aiming at the maximizing monomer conver-

\*To whom correspondence should be addressed.

sion, minimizing the side product concentration, or improving the property of final products have been conducted by Ray and Gupta<sup>16</sup> and Kumar and Sainath,<sup>17</sup> respectively. The former authors used temperature as a control variable, while the latter employed both temperature and pressure as control variables. Frontini et al.<sup>18</sup> have proposed optimal periodic control policies of monomer and initiator feed flows for anionic polymerization of isoprene.

Although theoretical optimization policies have been presented for many polymerization systems, very few of them have considered the diffusion-controlled free radical polymerization which accounts for both gel and glass effects.<sup>11</sup> Most previous work dealt with a kinetic model with an added gel effect into the kinetic expression. The model was proposed by Sacks et al.<sup>3</sup> and is expressed as

$$\frac{d\alpha}{dt} = \left( \frac{2fk_d I}{k_{t0}} \right)^{1/2} k_p \frac{(1-\alpha)}{g(\alpha)} + \frac{2fk_d I}{M_0} \quad (1)$$

where  $k_{t0}$  is the true termination constant,  $g(\alpha)$  represents the effect of molecular diffusion on termination rate,  $I$  is the initiator concentration, and  $M_0$  is the initial monomer concentration. This model usually leads to dead-ending polymerizations and leaves reaction incomplete due to the early depletion of initiators. In this case, the optimal temperature profile to minimize either the reaction time or the MWD is an increasing curve.<sup>3,10</sup> Sacks et al.<sup>10</sup> simplified the expression of the objective function for the minimum MWD problem inadvertently by using a constant ultimate number average chain length at each iteration in the boundary iteration solution scheme.<sup>19</sup> Based on their subsequent theoretical derivations, they concluded that for the minimum MWD problem the instantaneous number average molecular weight should be a constant along the optimal profile. As we shall see later, this criterion does not hold.

In bulk free radical polymerizations, the "gel effect" or the "Trommsdorf effect," which results from diffusion-controlled termination reactions among the large polymer radicals and may cause the autoacceleration of the polymerization rate, must be accounted for. In addition, the propagation rates may also become diffusion-controlled at high conversions when the polymerization temperature is below the glass transition temperature of the polymer being synthesized. For a typical free radical bulk homopolymerization such as a chemically initiated styrene reaction, the reaction rate decreases in the early period of reaction due to the consumption of monomers, then climbs up to the second maximum point due to the gel effect. Finally, the reaction rate decays rapidly to zero because of the glass effect. There is also a transition period between the regions of the gel effect and the glass effect, which is the so-called limited gel effect region.<sup>20</sup> The reaction rate is lower in the limited gel effect region than in the gel effect period.

The gel and the glass effects have often been accounted for by empirical correlations of the rate constants with conversion.<sup>3,21</sup> Recently, more fundamental approaches using free volume theory or de Gennes' reptation theory have been quite successful to model these effects for homopolymers<sup>20,22-30</sup> and

for copolymers.<sup>30,31</sup> However, they have seldom been applied in the open-loop optimal control of free radical polymerizations.

The purpose of this paper is threefold. First, the open-loop optimal temperature control by using the kinetic model proposed by Sacks et al.<sup>3</sup> is reworked using the variational method. The criterion of the minimum MWD policy is clarified in this study. Second, a kinetic-diffusion model incorporating both the gel and glass effects for the complete reaction course is used in the open-loop optimal temperature controls for batch homogeneous free radical polymerizations. The optimal temperature profiles to minimize reaction time or molecular weight distribution are presented. Physical aspects implied by these optimal temperature programs are elucidated as well. Third, experimental verifications of optimal temperature policies using the kinetic-diffusion model are carried out.

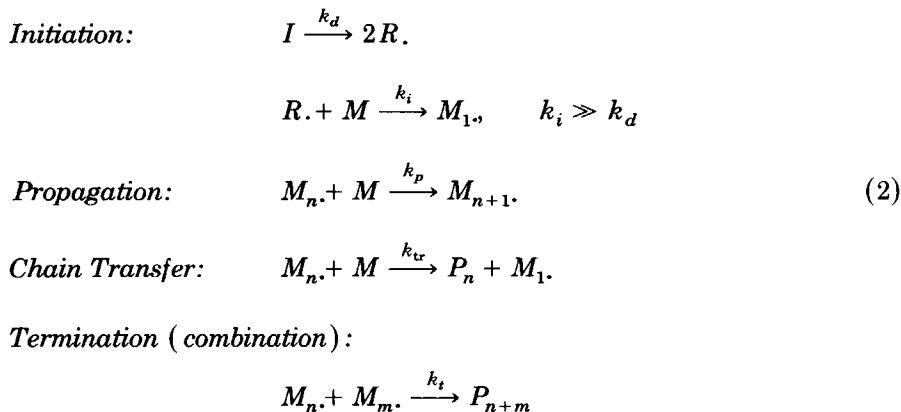
For open-loop optimal control (functional optimization, optimum programming, or dynamic optimization) problems, which arise in connection with processes developing in time or space, one or more control variables must be programmed to achieve certain terminal conditions. The problem is to determine, out of all possible programs for the control (decision, or manipulated) variables, the one program that minimizes (or maximizes) one terminal quantity while simultaneously yielding specified values of certain other terminal quantities. A most recent review on open-loop optimal control was given by Huang.<sup>19</sup>

To derive theoretical optimal policies in the research area of polymerizations, such methods as Pontryagin's maximum principle,<sup>2-7,10</sup> pattern search techniques,<sup>9,11</sup> or steepest descent method<sup>16,17</sup> have been employed. The steepest descent method is a control vector iteration approach to solve classical variational problems. The problem formulation allows one to include terminal constraints and stopping condition in addition to the objective function. This method starts with a nominal (nonoptimum) control variable program, and then improves this program in steps, using information obtained by a mathematical diagnosis of the program for the previous step. Conceptually, it is a process of local linearization around the path of the previous step. For optimization problems having terminal constraints and unspecified final time, although simultaneous optimization and collocation methods<sup>32,33</sup> can possibly be applied and still be powerful, Huang<sup>19</sup> has shown that the Slope Min-H strategy<sup>34</sup> along with the steepest descent method<sup>35</sup> is very useful in handling them. According to Denn,<sup>36</sup> the basic theoretical and computational framework for solving the optimization problems by variational methods has been unchanged over the past 25 years. Considerable insight into the structure of a problem can be obtained by the use of optimization techniques in conjunction with a process model that contains the significant qualitative features of the real system. For most applications the modern optimization methods can be an important tool for guidance to the designer.

## KINETICS

A generally accepted reaction mechanism for chemically initiated free radical bulk polymerization of styrene can be represented by the following

reactions:



The mechanism consists of chemical initiation by an irreversible initiator decay of a first order to produce primary radicals  $R.$ , first order propagation with respect to monomer  $M$ , first order chain transfer to monomer with respect to monomer, and second order termination by combination. The principle of equal reactivity of growing chains is assumed.

A kinetic-diffusion model developed in a previous work<sup>30</sup> is used here, which can be expressed by a single equation as follows:

$$\frac{d\alpha}{dt} = \frac{1 - \alpha}{\left(1 / \sqrt{\pi_1 + (\pi_2 \pi_3)^2 + \pi_2 \pi_3}\right) + \pi_4} \quad (3)$$

where  $\pi_1$  represents kinetic effect on propagation and termination for the conventional kinetics region,  $\pi_2$  and  $\pi_3$  denote diffusion effect on termination and kinetic effect on propagation respectively for the gel effect affected region, and  $\pi_4$  accounts for diffusion effect on propagation during the vitrification affected region. This model has been used to describe the styrene and unsaturated polyester polymerizations<sup>30</sup> and the curing process of SMC molding and vinyl casting.<sup>37</sup>

### OPTIMIZATION

A question we would like to raise now is what the optimal temperature profiles would be in order not only to minimize reaction time or molecular weight distribution but also to satisfy the ultimate monomer conversion and cumulative number average molecular weight for the corresponding isothermal condition. The formulation of the minimum reaction time problem will be discussed first, followed by the minimum MWD problem. In each case, two kinetic models [i.e., eqs. (1) and (3)] are considered. Only the formulation using kinetic model with both the gel and the glass effects will be shown here. The algorithms for the general optimization problem by using steepest descent<sup>35</sup> for the first stage of computation and Slope Min-H<sup>34</sup> as the final scheme will be followed.

### Minimization of Reaction Time

We would like to determine the temperature profile  $T(t)$  in the interval  $0 \leq t \leq t_f$ , so as to minimize the objective function, which is reaction time  $t_f$ :

$$\phi = t_f \quad (4)$$

The final time,  $t_f$ , is determined by the stopping condition

$$\Omega = \alpha(t_f) - \alpha^* = 0 \quad (5)$$

where  $\alpha^*$  is the final specification of monomer conversion.

The state equations accounting for both the gel and glass effects for the minimum reaction time problem are

$$\frac{d\alpha}{dt} = f_1(I, \alpha, T) = \frac{1 - \alpha}{\left(1/\sqrt{\pi_1 + (\pi_2\pi_3)^2 + \pi_2\pi_3}\right) + \pi_4} \quad (6)$$

$$\frac{dI}{dt} = f_2(I, \alpha, T) = -k_d I + \frac{\epsilon I}{1 - \epsilon\alpha} \frac{d\alpha}{dt} \quad (7)$$

$$\begin{aligned} \frac{d\mu_0}{dt} = f_3(I, \alpha, \mu_0, T) = & f k_d I + C_M \frac{[M_0]}{1 - \epsilon\alpha} \frac{d\alpha}{dt} \\ & + \frac{\mu_0 \epsilon (d\alpha/dt)}{1 - \epsilon\alpha} \end{aligned} \quad (8)$$

$$\begin{aligned} \frac{d\mu_1}{dt} = f_4(I, \alpha, \mu_1, T) = & k_t \lambda_0 \lambda_1 + k_{tr} \frac{[M_0](1 - \alpha)}{(1 - \epsilon\alpha)} \lambda_1 \\ & + \frac{\mu_1 \lambda_0 \epsilon (1 - \alpha)}{(1 - \epsilon\alpha)} k_p \end{aligned} \quad (9)$$

where  $\mu_i$  and  $\lambda_i$  are the  $i$ th moments of dead polymers and free radicals, respectively,  $C_M$  is the chain transfer constant to monomers, and  $\epsilon$  is the volume contraction factor.

The corresponding initial conditions are

$$I(0) = I_0, \quad \alpha(0) = \mu_0(0) = \mu_1(0) = 0 \quad (10)$$

The terminal condition is the specification of the ultimate cumulative number average molecular weight,  $\langle \bar{X}_n \rangle^*$

$$\psi = \left( \frac{1}{\mu_1/\mu_0} - \frac{1}{\langle \bar{X}_n \rangle^*} \right) \langle \bar{X}_n \rangle^* = 0 \quad (11)$$

Detailed numerical derivation of the optimization scheme is given elsewhere.<sup>19</sup>

### Minimization of MWD

The objective here is to determine the temperature profile  $T(t)$  in the interval  $0 \leq t \leq t_f$ , so as to minimize the objective function, which is the ultimate molecular weight distribution (MWD). The cumulative polydispersity is used here as an index for the MWD. For the minimum MWD problem, both models entail another state equation describing the second moment of the polymer distributions, and its corresponding Green's functions equation.

The objective function is the ultimate MWD. A general form is used here

$$\phi = \mu_0(t_f)\mu_2(t_f)/\mu_1^2(t_f) \quad (12)$$

The stopping and terminal conditions are the same as eqs. (5) and (11), respectively. The state equations by employing the kinetic model with both the gel and the glass effects are those in eqs. (6) to (9) together with the one describing the second moment of dead polymers:

$$\begin{aligned} \frac{d\mu_2}{dt} &= f_6(I, \alpha, \mu_2, T) \\ &= k_t(\lambda_2\lambda_0 + \lambda_1^2) + k_{tr} \frac{[M_0](1-\alpha)}{(1-\epsilon\alpha)}\lambda_2 + \frac{\mu_2\lambda_0\epsilon(1-\alpha)}{(1-\epsilon\alpha)}k_p \quad (13) \end{aligned}$$

with the initial conditions

$$I(0) = I_0, \quad \alpha(0) = \mu_0(0) = \mu_1(0) = \mu_2(0) = 0 \quad (14)$$

By following the similar procedures for the minimization of reaction time, the problem for the minimization of MWD can be readily formulated. Details are given elsewhere.<sup>19</sup>

The computing procedures for the steepest descent and the Slope Min-H have been discussed in details by Bryson and Denham<sup>35</sup> and Gottlieb<sup>34</sup> respectively. Detailed solution procedures and numerical techniques used in this work are given elsewhere.<sup>19</sup>

### MODEL PREDICTIONS

Bulk styrene polymerizations are used as examples here. The cases for the optimization study are summarized in Table I. The kinetic model with only the gel effect was used in case 1, while the model accounting for both the gel and glass effects was employed in case 2. For each case, both the minimum time and the minimum MWD problems were investigated. The corresponding isothermal conditions that achieved the specified ultimate monomer conversion,  $\alpha^*$ , and final cumulative number average chain length  $\langle \bar{X}_n \rangle^*$  (case 1) or molecular weight  $\langle \bar{M}_n \rangle^*$  (case 2) with the indicated initial initiator concentrations  $[I_0]$  are displayed in the table.  $[I_0]$  and  $T$  were chosen so that case 1 shows dead-ending polymerization, and case 2 shows conventional polymerization with both the gel effect and the glass effect.

TABLE I  
Summary of Case Studies for the Optimization

	Systems	$[I_0]$	$\alpha^*$	$\langle \bar{X}_n \rangle^*$ or $\langle \bar{M}_n \rangle^*$	Isothermal	Problem
Case 1 (a)	ST + AIBN	0.00806M	0.5	1181.0	71.8°C	Min time
(b)	—	—	—	—	—	Min MWD
Case 2 (a)	ST + BPO	0.1082M	0.98	13431.76	100.0°C	Min time
(b)	—	—	—	—	—	Min MWD

### Optimization Using Model with the Gel Effect Only

The kinetic data<sup>3</sup> that were used are summarized in Table II. The onset point of the gel effect has been modified slightly. Case 1 dealt with AIBN-initiated styrene reactions. The ultimate monomer conversion level was set at 0.5 and the final cumulative number average chain length at 1181. The isothermal profiles of kinetic characteristics such as molecular weights, polydispersity, monomer and initiator conversions, and reaction rate for monomer conversion, corresponding to case 1 are shown in Figures 1(a) and 1(b).

The isothermal reaction corresponding to case 1 shows the behavior of dead end polymerization [see Fig. 1(b)] since the ultimate initiator conversion exceeds 0.9, while the ultimate monomer conversion only reaches a level of 0.5. The reaction rate profile in the same figure exhibits a drastic decay due to the dead ending during the reaction course, although the gel effect occurring after a conversion of 0.3 somewhat moderates the decay. Figure 1(a) shows that both the instantaneous number average chain length and the cumulative polydispersity experience great increases, especially after a conversion of 0.3. For the minimization of reaction time, Figure 2(b) shows that the optimal rate profile is to decrease the reaction rate, relative to the isothermal one, before the on-set of gel effect, and to increase the rate after that [compare Figs. 1(b) and 2(b)]. It turns out that the optimal temperature profile shows a gradual increase throughout the reaction [see Fig. 2(a)]. The temperature which is lower than the isothermal case in the early stage of the reaction is to compensate for the decrease of molecular weight that would occur when the

TABLE II  
Kinetic Data for Model with Gel Effect (Styrene)<sup>3</sup>

$A_p$ (L s <sup>-1</sup> mol <sup>-1</sup> )	$1.051 \times 10^7$
$A_t$ (L s <sup>-1</sup> mol <sup>-1</sup> )	$1.255 \times 10^9$
$A_d$ (s)	$1.58 \times 10^{15}$
$E_p$ (cal mol <sup>-1</sup> )	7060
$E_t$ (cal mol <sup>-1</sup> )	1680
$E_d$ (cal mol <sup>-1</sup> )	30800
	1.0
$g = (k_t/k_{t0})^{1/2}$	$0 \leq \alpha \leq 0.2871$
	$1.522-1.818\alpha$
	$0.2871 \leq \alpha \leq 0.8$
$\eta, k_{tc}/k_t$	1.0
$f$	0.5
$[M_0]$	8.7

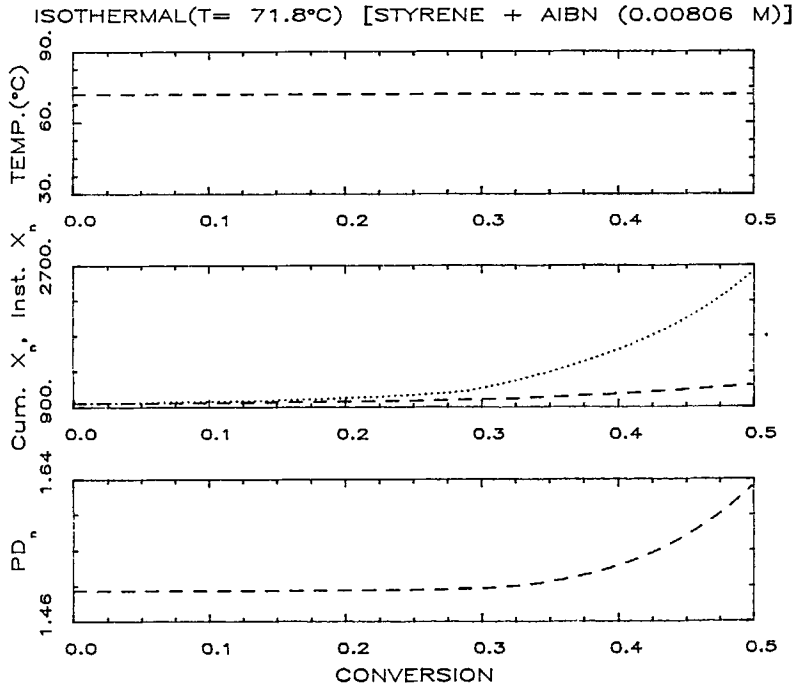


Fig. 1(a). Temperature, molecular weights, and polydispersity profiles of AIBN-initiated styrene reaction at  $T = 71.8^\circ\text{C}$  with  $[I_0] = 0.00806M$ ,  $\alpha^* = 0.5$ . ( $\cdots$ ) Inst.  $\bar{X}_n$ ; ( $---$ ) Cum.  $\bar{X}_n$ .

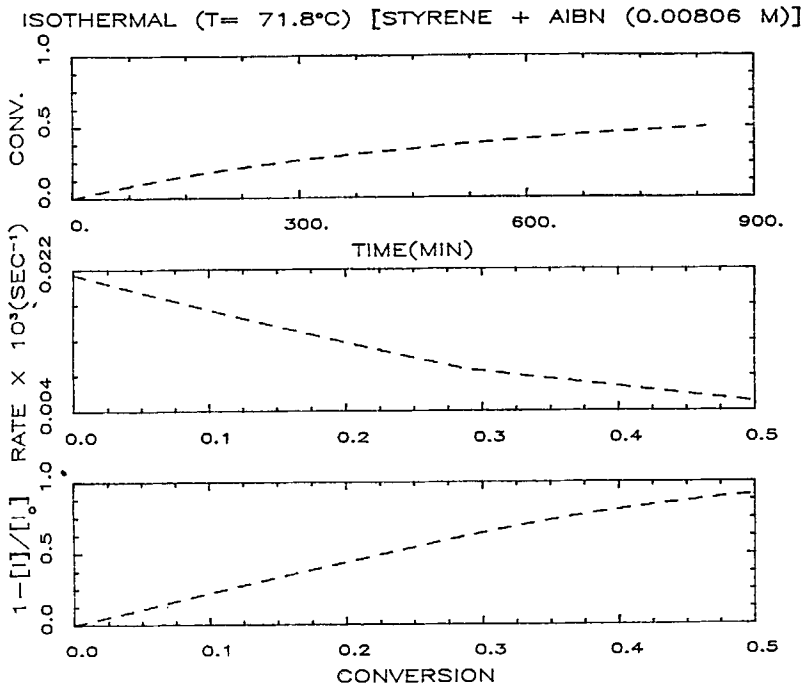


Fig. 1(b). Monomer conversion, reaction rate, and initiator conversion profiles of AIBN-initiated styrene reactions at  $T = 71.8^\circ\text{C}$  with  $[I_0] = 0.00806M$ ,  $\alpha^* = 0.5$ .



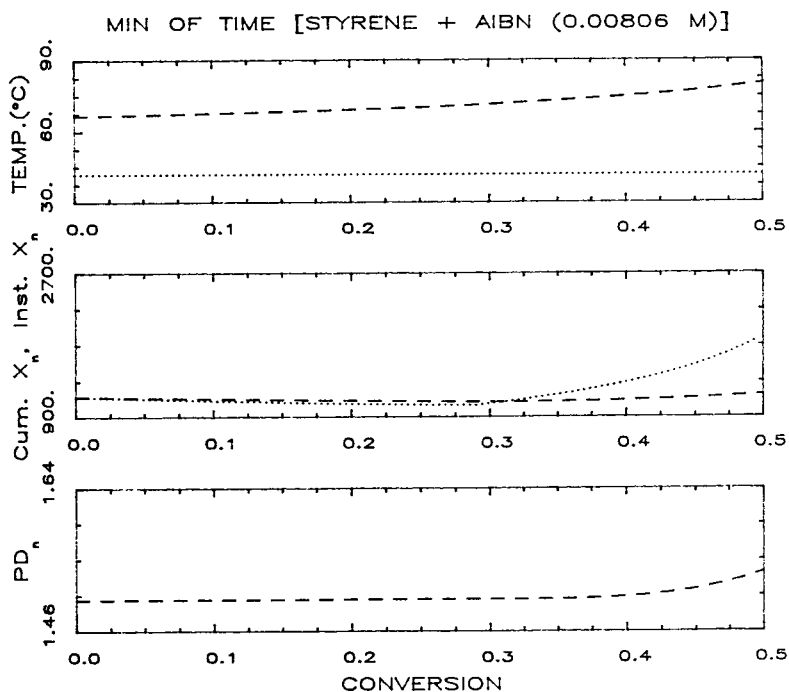


Fig. 2(a). Optimal temperature, molecular weights, and polydispersity profiles of AIBN-initiated styrene reactions with  $[I_0] = 0.00806M$  to minimize the reaction time with the target  $\alpha^* = 0.5$  and  $\langle \bar{X}_n \rangle^* = 1181.0$  [case 1(a)]. (· · ·) Initial temperature.

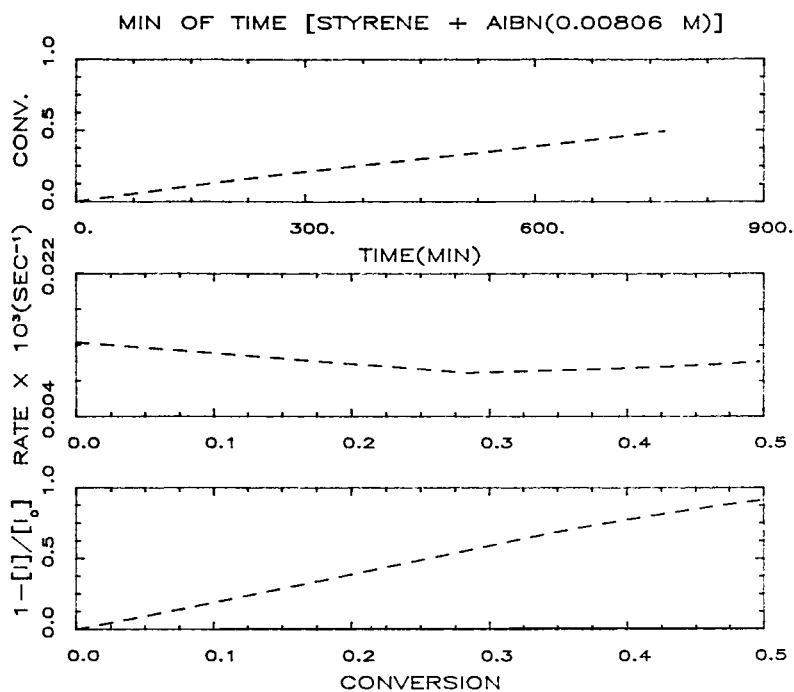


Fig. 2(b). Optimal monomer conversion, reaction rate, and initiator conversion profiles of AIBN-initiated styrene reactions with  $[I_0] = 0.00806M$  to minimize the reaction time with the target  $\alpha^* = 0.5$ , and  $\langle \bar{X}_n \rangle^* = 1181.0$  [case 1(a)].

TABLE III  
 Comparison of Isothermal, Nominal, and Optimum Results and Parameters  
 from Computer Simulation of AIBN-Initiated Styrene Reactions with  
 $[I_0] = 0.00806M$ ,  $\alpha^* = 0.5$ , and  $\langle \bar{X}_n \rangle^* = 1181.0$  (Case 1)

Case 1	Isothermal	(a) (min time)		(b) (min MWD)	
		Nominal	Optimum	Nominal	Optimum
Temp ( $^{\circ}C$ )	71.8	41.8	Fig. 3(a)	56.8	Fig. 4(a)
$[I_0]$ (M)	0.00806	0.00806	0.00806	0.00806	0.00806
$\alpha^*$	0.5	0.5	0.5	0.5	0.5
$\langle \bar{X}_n \rangle^*$	—	—	1181.0	—	1181.0
$\langle \bar{X}_n \rangle_{t=t_f}$	1181.25	3031.97	1181.00	1737.70	1181.08
$\overline{PD}_n (t = t_f)$	1.63	1.51	1.53	1.51	1.51
$\overline{PD}_n$ (% decrease)	—	—	—	—	8.54%
$c (= 1 - I/I_0)_{t=t_f}$	0.915	—	0.9140	—	0.9156
Reaction time (min)	846.12	10909.33	773.04	2570.01	798.90
Time saving (%)	—	—	9.45%	—	—
Convergence check $ \delta T _{\max}$ ( $^{\circ}C$ )	—	—	$2.55 \times 10^{-2}$	—	$3.27 \times 10^{-4}$
No. of iteration	—	—	56	—	34
Vax 8500 CPU time (min)	—	—	9	—	2

temperature is increased at the later reaction step. For the dead end polymerization, the instantaneous number average molecular weight will rise rapidly and the MWD will become broader after the onset of gel effect. The optimal temperature program depresses such increases because the molecular weight decreases as temperature increases [compare Figs. 1(a) and 3(a)]. The time saving as a result of optimal temperature policy, relative to the isothermal case, is 9.5%. Table III shows more details for the results.

The optimal temperature profile to minimize the reaction time also reduces the MWD for reactions characterized by dead end phenomena, but does not minimize the MWD. Although the optimal temperature profile to minimize the MWD shown in Figure 3(a) is again an increasing curve, it reveals distinct features. Prior to a monomer conversion of 0.3, it shows a slight increase to depress the deviation between the instantaneous and the cumulative number average molecular weights for the corresponding isothermal reaction [see Figs. 1(a) and 3(a)]. This is in contrast to the temperature profile to minimize the reaction time during the same period as shown in Figure 2(a), which increases in a slightly excessive manner that a reverse deviation between the two molecular weights results [compare Figs. 1(a), 2(a), and 3(a)]. After a conversion of 0.3 the optimal temperature is higher for the case of minimum MWD than for that of the minimum time in order to reduce the deviation of the two molecular weights to the least amount as possible in the corresponding isothermal reaction [compare Figs. 2(a) and 3(a)]. Alternatively, the difference between the two optimal temperature profiles can be clarified by comparing the optimal reaction rate profiles in Figures 2(b) and 3(b), respectively. These rate profiles reflect that lower temperatures in the early part and higher

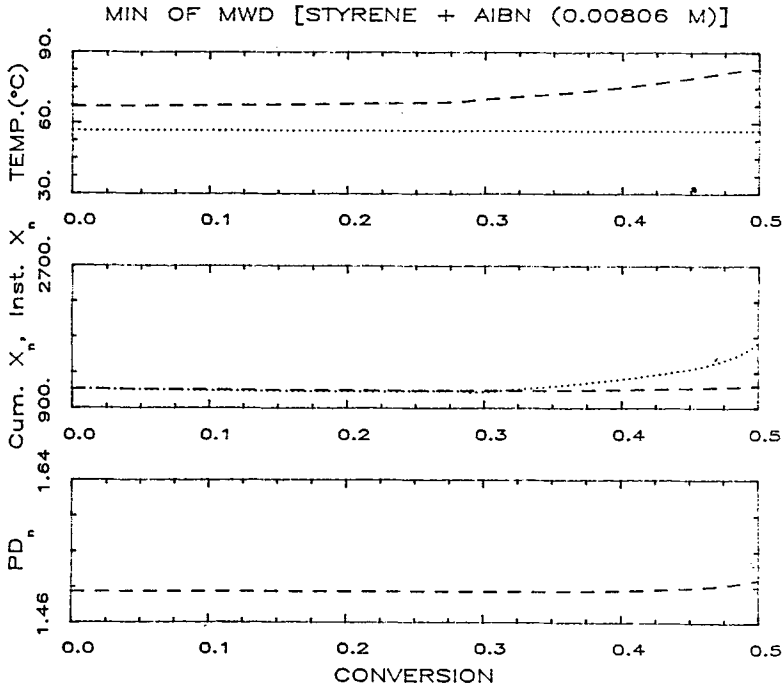


Fig. 3(a). Optimal temperature, molecular weights, and polydispersity profiles of AIBN-initiated styrene reactions with  $[I_0] = 0.00806M$  to minimize the molecular weight distribution (MWD) with the target  $\alpha^* = 0.5$ , and  $\langle \bar{X}_n \rangle^* = 1181.0$  [case 1(b)].

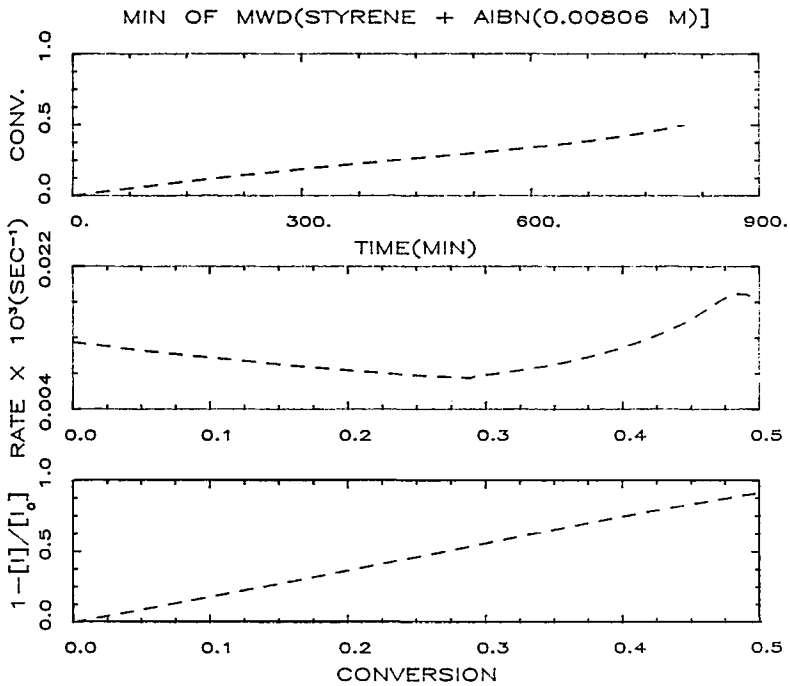


Fig. 3(b). Optimal monomer conversion, reaction rate, and initiator conversion profiles of AIBN-initiated styrene reactions with  $[I_0] = 0.00806M$  to minimize the molecular weight distribution (MWD) with the target  $\alpha^* = 0.5$ , and  $\langle \bar{X}_n \rangle^* = 1181.0$  [case 1(b)].

temperatures in the later part of the reaction must have been applied for the case of minimum MWD than those of the minimum time. Figure 3(a) discloses that a lower level of cumulative polydispersity, relative to that in Figure 2(a), results. A decrease in  $\overline{PD}_n$  under the optimal profile can be up to 8.54% when compared with the isothermal case as displayed in Table III.

### Optimization Using Model with Both the Gel and the Glass Effects

The numerical values of parameters for the kinetic model with both the gel and the glass effects are listed in Table IV. The isothermal profiles of molecular weights, conversions of monomer and initiator, and reaction rate relative to case 2 are shown in Figures 4(a) and 4(b). It dealt with a BPO-initiated styrene reaction at  $T = 100^\circ\text{C}$  with  $[I_0] = 0.1082M$ , an ultimate monomer conversion of 0.98, and a final  $\langle \overline{M}_n \rangle$  of 13,431.

Figure 4(b) shows that the polymerization exhibits the conventional behavior since the rate of initiator consumption is much lower than that of monomer consumption during reaction. Figure 4(a) shows that, for the conventional polymerization, the instantaneous number average molecular weight  $\overline{M}_n$  decreases with conversion prior to the onset of gel effect, but increases

TABLE IV  
Kinetic Data for Model with Both the Gel and the Glass Effects (Styrene)

#### a. Kinetics<sup>42</sup>

$$qz_0/2fI_0 = 0.0966 \text{ (isothermal)}$$

$$qz_0/2fI_0 = 0 \text{ (optimization studies)}$$

$$[I_0] = 0.1082M$$

$$q = f = 1.0$$

$$k_d \text{ (min}^{-1}\text{)} = 5.9 \times 10^{14} \exp(-28400/RT)$$

$$T_{gP} = 366.7 \text{ K}$$

$$T_{gM} = 185.0 \text{ K}$$

$$\beta_p = 0.00048$$

$$\beta_M = 0.001$$

$$\lambda = 1 \text{ for } T \geq 85^\circ\text{C}$$

$$\lambda = 0.3 \text{ for } T < 85^\circ\text{C}$$

$$d_p \text{ (g/cm}^3\text{)} = 1.084 - 0.000605(T - 273.2)$$

$$d_M \text{ (g/cm}^3\text{)} = 0.924 - 0.000918(T - 273.2)$$

$$2fI_0k_{p0}F \text{ (min}^{-1}\text{)} = 0.01 \exp(2681/RT)$$

$$2fI_0k_dk_{p0}^2/k_{t0} \text{ (min}^{-2}\text{)} = 1.8 \times 10^{23} \exp(-45214/RT)$$

$$A_M \text{ (min)} = 2.73 \times 10^{11} \exp(-27454/RT)$$

$$B_M = 0.42$$

$$B_p = 0.01837$$

$$A_p/F \text{ (min)} = \exp[a' + b'(\ln 1/V_f - \ln 1/\overline{V}_{f0}) + c'(\ln 1/V_F - \ln 1/\overline{V}_{f0})^2]$$

$$\text{where } a' = -14.83 + 6845/T$$

$$b' = -14.17 + 5213/T$$

$$c' = -8.56 + 2473/T$$

$$\ln 1/\overline{V}_{f0} = 3.2824$$

#### b. Molecular weights<sup>40</sup>

$$C_M = 1.00 \exp(-3212/T)$$

$$f = 1.0$$

$$[I_0] = 0.1082 \text{ mol/L}$$

$$[M_0] = 8.6635 \text{ mol/L}$$

$$k_{p0} = 7.138 \times 10^9 \exp(-5616/T) \text{ (s}^{-1} M^{-1}\text{)}^{41}$$

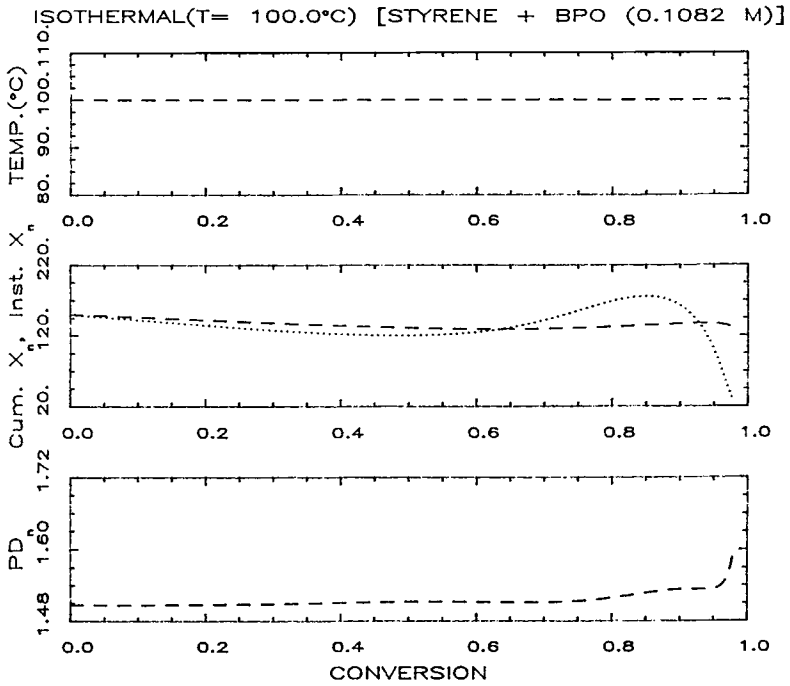


Fig. 4(a). Temperature, molecular weights, and polydispersity profiles of BPO-initiated styrene reactions at  $T = 100^\circ\text{C}$  with  $[I_0] = 0.1082\text{M}$ ,  $\alpha^* = 0.98$ .

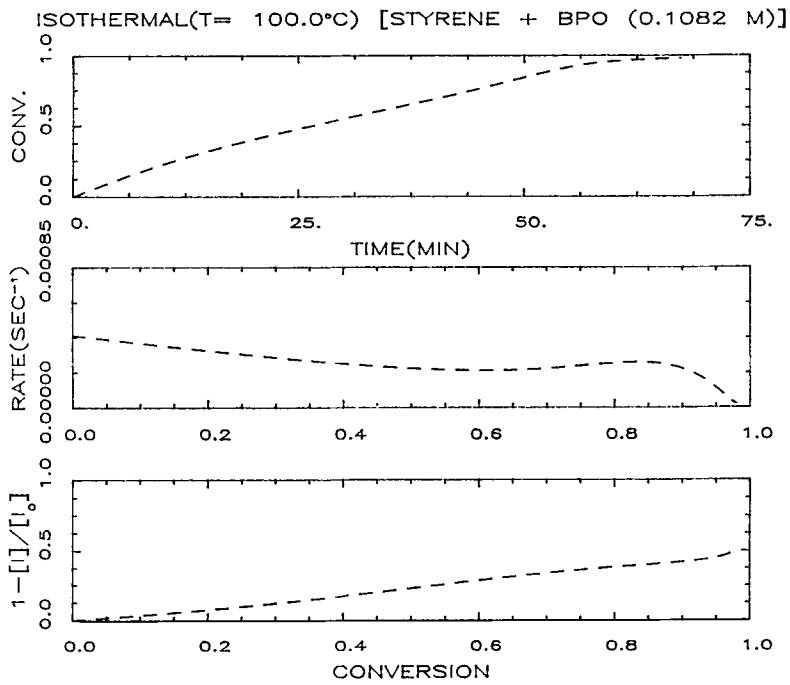


Fig. 4(b). Monomer conversion, reaction rate, and initiator conversion profiles of BPO-initiated styrene reactions at  $T = 100^\circ\text{C}$  with  $[I_0] = 0.1082\text{M}$ ,  $\alpha^* = 0.98$ .

during the gel effect region. It decreases somewhat in the limited gel effect region, followed by a rapid drop once the glass effect occurs.

Both the gel effect and the glass effect can result in an increase in the cumulative polydispersity, i.e., the broadening of the molecular weight distribution [see Fig. 4(a) for monomer conversion range of 0.8–0.9 and of 0.95–0.98, respectively], but for different reasons. The gel effect, which is due to diffusion-controlled termination, leads to more polymers having longer chains. The increase of weight average molecular weight is thus more enhanced than that of number average molecular weight. By contrast, the glass effect, which is due to diffusion-controlled propagation, causes more shorter chain polymers. Consequently, the decrease of number average molecular weights is much more marked than that of weight average molecular weights. In either case, the outcome of the MWD is the same.

The optimal temperature profile to minimize the reaction time starts with a constant temperature of 103.5°C until a conversion of 0.4, followed by a gradual decrease which passes 100°C at a conversion of 0.6 and reaches 95.5°C at a conversion of 0.8, and then maintains that level up to a conversion of 0.9. Finally, it increases gradually to 97°C at a conversion of 0.95, and rises rapidly to 104°C up to the final conversion of 0.98 [see Fig. 5(a)]. The physical aspect implied by the optimal temperature profile is that a temperature higher than the corresponding isothermal temperature (i.e., 100°C) is employed at the earliest possible time (i.e., for the conventional kinetic region up to a monomer conversion of 0.6), but a temperature lower than 100°C is required at the later

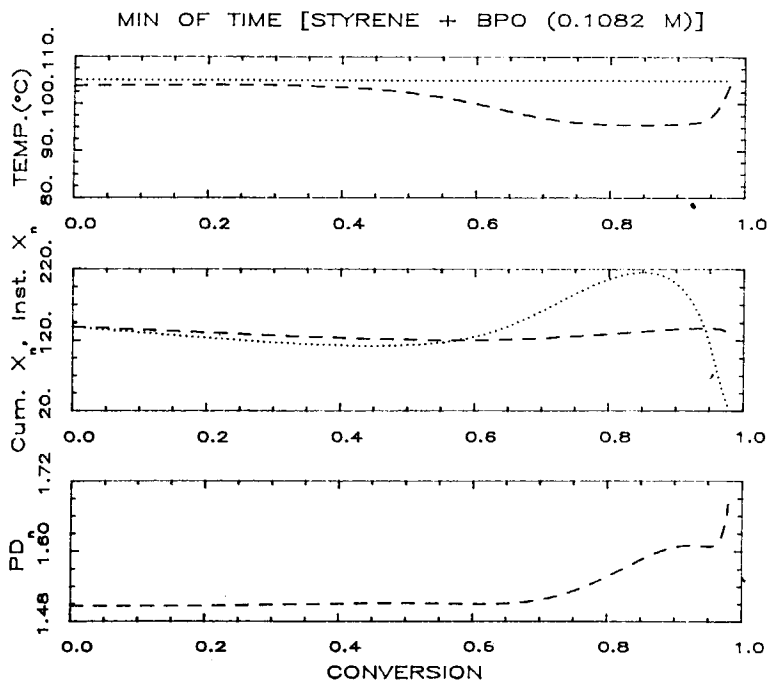


Fig. 5(a). Optimal temperature, molecular weights, and polydispersity profiles of BPO-initiated styrene reactions with  $[I_0] = 0.1082M$  to minimize the reaction time with the target  $\alpha^* = 0.98$ , and  $\langle \bar{M}_n \rangle^* = 13431.76$  [case 2(a)].

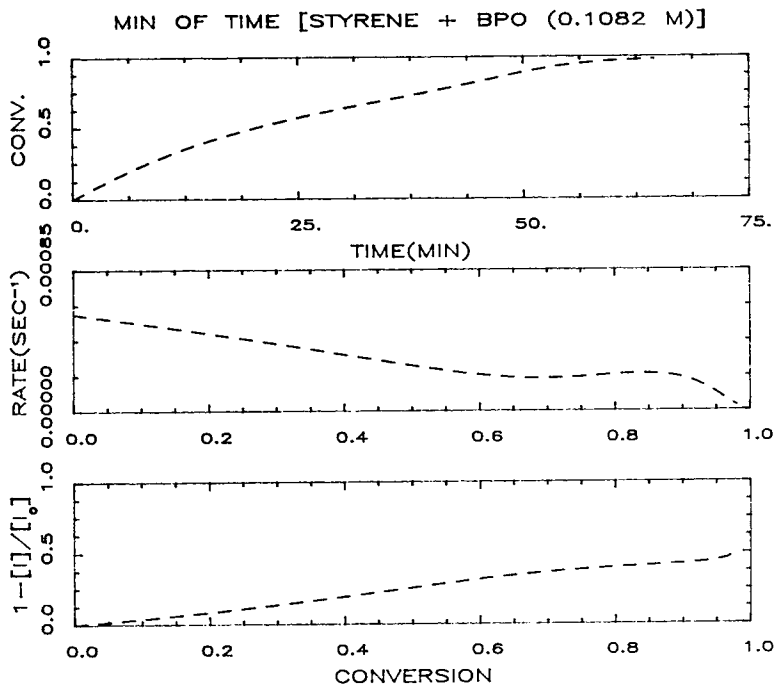


Fig. 5(b). Optimal monomer conversion, reaction rate, and initiator conversion profiles of BPO-initiated styrene reactions with  $[I_0] = 0.1082M$  to minimize the reaction time with the target  $\alpha^* = 0.98$ , and  $\langle \bar{M}_n \rangle^* = 13431.76$  [case 2(a)].

time [i.e., for the gel effect (0.6–0.9 conversion) and the limited gel effect (0.9–0.95 conversion) regions] to compensate for the deterioration of the molecular weights due to the higher temperature applied in the preceding step. Finally, higher temperature should be used (i.e., for the glass effect region from 0.95 to 0.98 conversion). For the last 8% of monomer conversion (i.e., 0.9–0.98 conversion), the first gradual temperature increase (i.e., from 0.9 to 0.95 conversion) is to shorten the reaction time during which the limited gel effect predominates, while the second sharp increase (i.e., from 0.95 to 0.98 conversion) is to reduce the time during which the glass effect is overwhelming. Since the reaction rate is much lower in the glass effect region than in the limited gel effect period, higher temperature is employed for the former period.

One should differentiate this case from case 1(a) where the reaction is of dead ending instead of conventional. For case 1(a), if higher temperatures had been applied in the early step, the specifications of ultimate monomer conversion would not have been achieved owing to the dead ending phenomenon. Therefore, the optimal policy is to start with a lower temperature and keep increasing the temperature till the end. For conventional polymerizations, the time saving due to the optimal temperature profile essentially originates from the first (kinetics-controlled) and last (vitrification-controlled) stages of the reaction. This is in contrast to the case of dead end polymerization where the saving mostly comes from the later stage (severe dead ending and gel effect).

TABLE V  
 Comparison of Isothermal, Nominal, and Optimum Results and Parameters  
 from Computer Simulation of BPO Initiated Styrene Reactions with  
 $[I_0] = 0.1082M$ ,  $\alpha^* = 0.98$ , and  $\langle \bar{M}_n \rangle^* = 13431.76$  (Case 2)

Case 2	Isothermal	(a) (min time)		(b) (min MWD)	
		Nominal	Optimum	Nominal	Optimum
Temp (°C)	100.0	105.0	Fig. 5(a)	105.0	Fig. 6(a)
$[I_0]$ (M)	0.1082	0.1082	0.1082	0.1082	0.1082
$\alpha^*$	0.98	0.98	0.98	0.98	0.98
$\langle \bar{M}_n \rangle^*$	—	—	13431.76	—	13431.76
$\langle \bar{M}_n \rangle_{t-t_f}$	13431.76	11481.18	13431.68	11481.18	13430.94
$\overline{PD}_n(t-t_f)$	1.60	1.58	1.68	1.58	1.54
$\overline{PD}_n$ (% decrease)	—	—	—	—	3.4%
$c = (1 - I/I_0)_{t-t_f}$	0.5123	—	0.5114	—	0.5124
Reaction time (min)	67.44	54.16	64.56	54.16	72.53
Time saving (%)	—	—	4.46%	—	—
Convergence check $ \delta T _{\max}$ (°C)	—	—	$7.51 \times 10^{-4}$	—	$4.60 \times 10^{-4}$
No. of iteration	—	—	24	—	25
Vax 8500 CPU time (min)	—	—	4	—	8

Table V shows that a time saving of 4.46% is obtained as a result of the optimal policy when compared with the isothermal case. Although the reaction time is minimized, the ultimate cumulative polydispersity increases greatly [compare Figs. 4(a) and 5(a)].

To minimize the MWD, Figure 6(a) shows that the optimal temperature follows a decreasing temperature strategy up to 60% conversion. It starts with a temperature of 108°C, passes 100°C at a conversion of 0.3, and reaches 98°C at about 60% conversion. Subsequently, it increases gradually from 98°C to 105°C at a conversion of 0.8, followed by a decrease to 91°C up to a conversion of 0.95. From the conversion of 0.95–0.98, the temperature increases slightly from 91 to 93°C. The basic principle of MWD minimization is to minimize the deviation between the instantaneous and the cumulative number average molecular weights for the corresponding isothermal reaction. The isothermal profiles of the molecular weights in Figure 4(a) show that deviations between the two molecular weights exist for the entire reaction. In the kinetics-controlled region up to a conversion of 0.6, the deviation is minor. It becomes severe in the gel effect region from a conversion of 0.6–0.9. Although the deviation is reduced appreciably in the limited gel effect region from a conversion of 0.9–0.95, a great deviation develops in the glass effect region from a conversion of 0.95–0.98. To correct the deviations between the two molecular weights, the optimal temperature profile follows exactly the way the instantaneous molecular weight varies in the corresponding isothermal reaction [compare Figs. 4(a) and 6(a)]. Prior to 95% conversion, all the temperature variations to remedy the deviations are based on the fact that the instantaneous number average molecular weight is a decreasing function



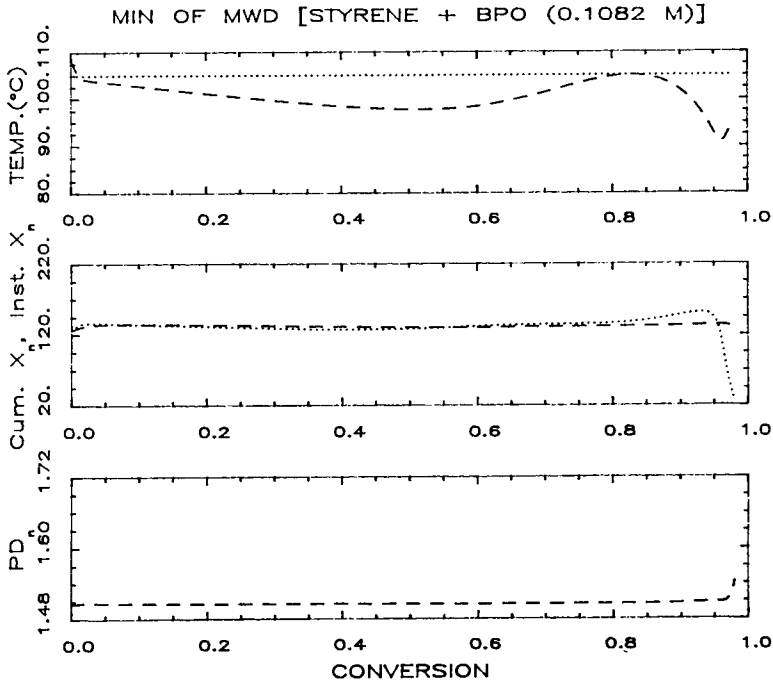


Fig. 6(a). Optimal temperature, molecular weights, and polydispersity profiles of BPO-initiated styrene reactions with  $[I_0] = 0.1082M$  to minimize the molecular weight distribution (MWD) with the target  $\alpha^* = 0.98$ , and  $\langle \bar{M}_n \rangle^* = 13431.76$  [case 2(b)].

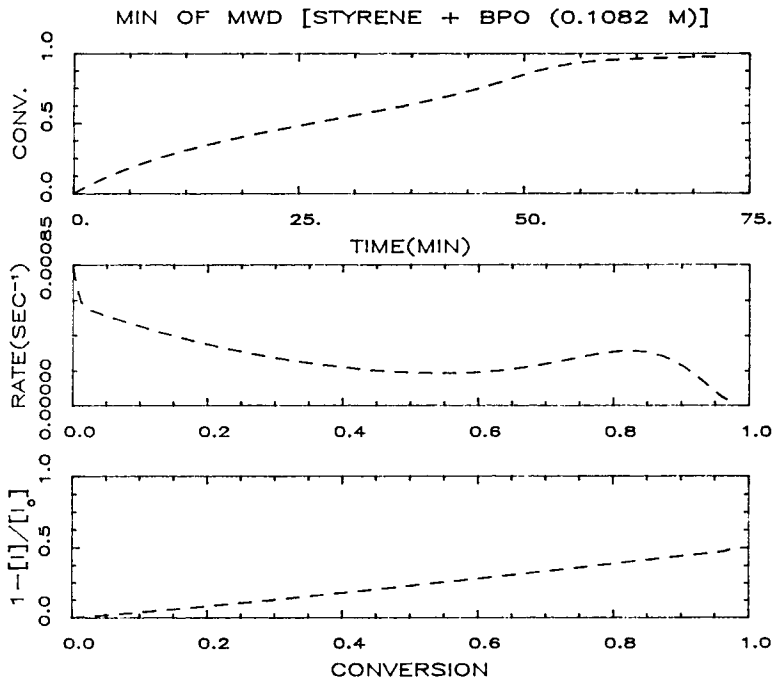


Fig. 6(b). Optimal monomer conversion, reaction rate, and initiator conversion profiles of BPO-initiated styrene reactions with  $[I_0] = 0.1082M$  to minimize the molecular weight distribution (MWD) with the target  $\alpha^* = 0.98$ , and  $\langle \bar{M}_n \rangle^* = 13431.76$  [case 2(b)].

of temperature. However, as the glass effect sets in, lowering temperatures will further restrict the monomer mobilities in the propagation step, and, in turn, decrease the instantaneous number average molecular weight. Therefore, to reduce the limitation of propagation due to the glass effect, the optimal temperature profile from a conversion of 0.95–0.98 is to raise the temperature from 91 to 93°C as shown in Figure 6(a). As a consequence of the optimal profile, the ultimate cumulative polydispersity decreases by 3.4% when compared with the isothermal reaction [see Table V, and compare Figs. 4(a) and 6(a)]. However, the reaction time is prolonged. Table V shows an increase of 5 min in reaction time, which is 7.5% more than the time required by the isothermal reaction.

### EXPERIMENTAL VERIFICATIONS

Experimental verifications of the optimal temperature profiles to minimize the reaction time and MWD were conducted for styrene polymerization initiated by benzoyl peroxide (BPO). Styrene was first freed of inhibitor by the usual procedures. Three parts of initiator, BPO, and 0.26 part of benzoquinone (BQ) were then added to the 100 parts of monomer. Thirty to 45 mg of sample were put into a preweighed stainless steel pan and loaded into a differential scanning calorimeter (DSC-2C, Perkin-Elmer). At a heating or cooling rate of 320°C/min, the DSC was employed to simulate the optimal temperature profiles by a piecewise temperature change for every 2 min using manual control. The equilibrium time during the temperature changeover was less than 1 min. At nominal conversions of 20, 40, 60, 80, 90, or 100% determined by the reaction times from the theoretical prediction, the sample pan was removed and quickly quenched with ice. Two such cured samples for each nominal conversion were prepared for subsequent conversion and molecular weight measurements.

One cured sample was then reheated from 40 to 200°C in the scanning mode of DSC with a heating rate of 5°C/min to determine the residual exotherm left. The total heat of reaction was calculated from areas under both DSC curves, and the conversion of the partially cured sample was readily obtained.<sup>19</sup> The other partially cured sample was dissolved in chloroform (0.04 mL/mg polymer) and the polymer was precipitated in excess chilled methanol (0.2 mL/mg polymer).<sup>38</sup> The polymer was separated from the solution by centrifuging at 3300 rpm for about 30 min, and the recovered wet cake of polymer was air dried overnight. Polymer solution (0.1 wt %) in tetrahydrofuran was prepared. The molecular weights and molecular weight distribution were then measured by a gel permeation chromatograph (GPC, Waters) with a Rheodyne 7010 sample injection valve, a Model 6000A solvent delivery system, four ultrastyrigel columns ( $10^2$ ,  $10^3$ ,  $10^4$ , and  $10^5$  Å pore sizes), and a Model 410 differential refractometer.

### RESULTS AND DISCUSSIONS

Three sets of experiments using the isothermal temperature (100°C), optimal temperature policies for minimum time [i.e., Fig. 5(a)] and minimum

TABLE VI  
Comparison of Experimental and Calculated Conversion and Molecular Weights Histories under Isothermal Temperature (100°C)

Time (min)	Conversion		$\langle \bar{M}_n \rangle$		$\overline{PD}_n$	
	(Exptl)	(Calcd)	(Exptl)	(Calcd)	(Exptl)	(Calcd)
9.65	0.324	0.221	12850	14698	1.81	1.51
20.65	0.482	0.415	15730	13912	1.63	1.51
34.65	0.645	0.615	15519	13444	1.76	1.51
48.65	0.864	0.821	18596	13925	1.87	1.52
56.65	0.951	0.936	16097	14301	2.06	1.53
67.25	1.0	0.980	18351	13450	2.10	1.60

TABLE VII  
Comparison of Experimental and Calculated Conversion and Molecular Weights Histories under Optimal Temperature Policy for Minimum Reaction Time

Time (min)	Conversion		$\langle \bar{M}_n \rangle$		$\overline{PD}_n$	
	(Exptl)	(Calcd)	(Exptl)	(Calcd)	(Exptl)	(Calcd)
6.65	0.340	0.208	12034	13589	1.77	1.51
14.65	0.505	0.399	12936	12862	2.10	1.51
27.65	0.654	0.609	15408	12543	1.73	1.51
43.65	0.829	0.805	17350	13506	1.94	1.56
51.65	0.888	0.909	18378	14233	2.09	1.61
64.45	0.996	0.980	19524	13449	2.06	1.68

TABLE VIII  
Comparison of Experimental and Calculated Conversion and Molecular Weights Histories under Optimal Temperature Policy for Minimum Molecular Weight Distribution (MWD)

Time (min)	Conversion		$\langle \bar{M}_n \rangle$		$\overline{PD}_n$	
	(Exptl)	(Calcd)	(Exptl)	(Calcd)	(Exptl)	(Calcd)
6.94	0.275	0.200	12266	13930	1.77	1.51
18.94	0.518	0.407	14875	13657	1.70	1.51
34.94	0.654	0.606	15806	13578	1.76	1.51
47.94	0.826	0.810	18591	13691	1.84	1.51
52.94	0.948	0.902	19550	13807	1.88	1.51
72.33	0.998	0.980	18773	13441	1.99	1.54

MWD [i.e., Fig. 6(a)] were investigated following the procedures outlined above. A comparison of the experimental data and model predictions for conversion, cumulative number average molecular weight, and polydispersity at different reaction times is displayed in Tables VI–VIII for isothermal, minimum time, and minimum MWD strategies, respectively. As can be seen

from these tables, the experimental conversion data resulting from the thermal method are in good agreement with the model predictions except at low conversions in each case. However, the experimental cumulative number average molecular weight and polydispersity data reveal some deviations in comparison with the calculated ones with most of the experimental data somewhat higher. The discrepancies between the experimental and calculated results for cumulative number average molecular weights and for polydispersity in particular could not be reduced too much even if experimental molecular weight data were employed in parameter fitting procedures during the development of the kinetic model for chemically initiated high conversion diffusion-controlled free radical polymerization systems.<sup>29,37</sup> In the optimization of high conversion thermal polymerization studies, Wu et al.<sup>7</sup> used a kinetic model proposed by Hui and Hamielec,<sup>39</sup> which was developed by using the experimentally determined conversion, and number and weight average molecular weights over the ranges of temperature and conversion investigated to fit parameters in the zeroth, first, and second moment equations for dead polymers. Therefore, it was quite accurate in predicting conversion and molecular weights. On the other hand, in the optimization of chemically initiated medium conversion free radical polymerization studies, Chen and Jeng<sup>4</sup> used a kinetic model developed by Sacks et al.,<sup>3</sup> which was developed by employing only the experimental conversion data to fit parameters in the rate equation for monomer. Moment equations for dead polymers were determined without resorting to any molecular weight data. The same principles have been adopted in developing our kinetic model. Consequently, it is not unexpected that model prediction was good for conversion but not as good for the molecular weights.

Although the absolute values of the predicted molecular weight and MWD deviate somewhat from the experimental data, the predicted improvements from the optimization policies show consistent trends. Under isothermal temperature policy, experimental data in Table VI indicate that, at the ultimate reaction time of 67.25 min, conversion, cumulative number average molecular weight, and polydispersity attain a level of 1.0, 18,351, and 2.1034, respectively. Table VII shows that the optimal temperature policy for minimum reaction time leads to an ultimate conversion of 0.996 and a number average molecular weight of 19,524 at the end of 64.45 min, with deviations in conversion and molecular weight being 0.4 and 6.4%, respectively, in comparison with the target values obtained from the isothermal experiment. On the other hand, Table VIII shows that the optimal temperature policy for minimum MWD results in final conversion, cumulative number average molecular weight, and polydispersity at a level of 0.998, 18,773, and 1.9939, respectively, at the end of 72.33 min. The conversion and the number average molecular weight deviate 0.2 and 2.3%, respectively, from the target values in the isothermal experiment. The decrease in polydispersity is 5.2%, which is very close to the theoretical prediction of 3.4% as shown in Table V. Therefore, despite the model validation by experiments being less than satisfactory, the trends of policy improvements for minimum reaction time and minimum MWD are consistent.

## CONCLUSIONS

The open-loop optimal temperature control or functional optimization problems for the batch free radical bulk polymerizations of styrene in lumped-parameter systems have been formulated by variational methods. Rational computational procedures which include the steepest descent method as the first phase and a Slope Min-H strategy as the final phase have been employed. The stopping condition and terminal constraints can be incorporated easily in the scheme in addition to the objective function. Both the minimum time and the minimum molecular weight distribution (MWD) problems can be solved numerically with very good convergence and short computing time.

For the minimum time problem, the optimal temperature program uses lower temperatures in the early stage and higher temperatures in the later stage for dead ending polymerizations. For conventional polymerizations, if the ultimate monomer conversion is high enough for the reaction to encounter an appreciable gel effect, the optimal temperature policy simply reverses the strategy used in the case of dead ending, i.e., higher temperature in early and lower temperature in later steps. If the glass effect exists as well, the optimal temperature policy in that period is to raise the temperature in order to mitigate the limitation of propagation due to vitrification.

For the minimum MWD problems, the optimal temperature policy is to minimize the deviations between the instantaneous and the cumulative number average molecular weights for the corresponding isothermal reaction. Sacks et al.<sup>10</sup> have used an inappropriate expression for the objective, and derived that the instantaneous number average molecular weight should be kept constant along the optimal path if the ultimate MWD is to be minimized. This assertion has been found incorrect in this work. The optimal temperature profile to minimize the ultimate MWD follows quite closely the variations of the instantaneous number average molecular weights under the corresponding isothermal condition. For dead ending polymerizations, under isothermal condition, the instantaneous number average molecular weight is essentially constant for the early stage and increases rapidly with conversion later when the dead ending phenomenon becomes severe. The optimal temperature policy uses essentially a constant temperature for the early stage, and employs an increasing temperature strategy to minimize the deviations of the two molecular weights. For conventional polymerizations, under isothermal condition, the instantaneous number average molecular weight decreases slowly in the kinetics-controlled region. It increases quite rapidly during the gel effect region, followed by a moderate decrease during the limited gel effect region, and finally ends up with a drastic drop. Since the deviations between the instantaneous and the cumulative number average molecular weights is basically reflected by the profile of the instantaneous number average molecular weight, the optimal temperature essentially follows this profile for the corresponding isothermal reaction except that in the glass effect region the optimal policy is to increase the temperature rather than to decrease it due to the reverse temperature dependency on molecular weights relative to the preceding regions.

In general, minimizing the reaction time does not guarantee that the ultimate MWD will be minimized simultaneously. It has been found that if one of the objectives is minimized, satisfying the other objective would usually become worse. For dead-ending polymerizations, minimizing the reaction time also greatly reduces the ultimate MWD. However, under no circumstances would both objectives be minimized simultaneously. Therefore, the assertion by Chen and Huang,<sup>6</sup> who claimed that, for dead-ending polymerizations, minimizing the reaction time would minimize the ultimate MWD as well, is incorrect in a strict sense.

DSC and GPC were employed to test the validity of the optimization results. Experimental verifications of optimal temperature profiles show that while the conversions of monomer during experiments are in reasonable agreement with predictions of the model, the cumulative number average molecular weight and polydispersity encounter some deviations. Nevertheless, the trends of policy improvements between the experimental work and the theory for chemically initiated high conversion diffusion-controlled free radical polymerizations in lumped-parameter systems are consistent.

### References

1. J. F. MacGregor, A. Penlidis, and A. E. Hamielec, *Polym Prod. Eng.*, **2**(2 & 3), 179 (1984).
2. Y. Yoshimoto, H. Yanagawa, T. Suzuki, T. Araki, and Y. Inaba, *Int. Chem. Eng.*, **11**, 147 (1971).
3. M. E. Sacks, S. I. Lee, and J. A. Biesenberger, *Chem. Eng. Sci.*, **27**, 2281 (1972).
4. S. A. Chen and W. F. Jeng, *Chem. Eng. Sci.*, **33**, 735 (1978).
5. S. A. Chen and K. F. Lin, *Chem. Eng. Sci.*, **35**, 2325 (1980).
6. S. A. Chen and N. W. Huang, *Chem. Eng. Sci.*, **36**, 1295 (1981).
7. G. Z. A. Wu, L. A. Denton, and R. L. Laurence, *Polym. Eng. Sci.*, **22**, 1 (1982).
8. S. A. Chen and K. Y. Hsu, *Chem. Eng. Sci.*, **39**, 177 (1984).
9. K. Osakada and L. T. Fan, *J. Appl. Polym. Sci.*, **14**, 3065 (1970).
10. M. E. Sacks, S. I. Lee, and J. A. Biesenberger, *Chem. Eng. Sci.*, **28**, 241 (1973).
11. B. M. Louie and D. S. Soong, *J. Appl. Polym. Sci.*, **30**, 3707 (1985).
12. S. A. Chen and S. T. Lee, *Polym. Eng. Sci.*, **25**, 987 (1985).
13. S. A. Chen and S. T. Lee, *Polym. Eng. Sci.*, **27**, 573 (1987).
14. A. Tsoukas, M. Tirrell, and G. Stephanopoulos, *Chem. Eng. Sci.*, **37**, 1785 (1982).
15. J. N. Farber, *Polym. Eng. Sci.*, **26**, 499 (1986).
16. A. K. Ray and S. K. Gupta, *Polym. Eng. Sci.*, **26**, 1033 (1986).
17. A. Kumar and A. E. Sainath, *Polym. Eng. Sci.*, **27**, 740 (1987).
18. G. L. Frontini, G. E. Elicabe, and G. R. Meira, *J. Appl. Polym. Sci.*, **33**, 2165 (1987).
19. Y. J. Huang, Ph.D. dissertation, The Ohio State University, 1987.
20. S. K. and D. C. Sundberg, *J. Polym. Sci. Polym. Chem. Ed.*, **20**, 1345 (1982).
21. J. F. Stevenson, *Polym. Eng. Sci.*, **26**(11), 746 (1986).
22. S. T. Balke and A. E. Hamielec, *J. Appl. Polym. Sci.*, **17**, 905 (1973).
23. J. N. Cardenas and K. F. O'Driscoll, *J. Polym. Sci. Polym. Chem. Ed.*, **14**, 883 (1976).
24. R. T. Ross and R. L. Laurence, *AIChE Symp. Ser.*, **72**, 80 (1976).
25. K. Arai and S. Saito, *J. Chem. Eng. Jpn.*, **9**(4), 302 (1976).
26. F. L. Marten and A. E. Hamielec, *Am. Chem. Soc. Symp. Ser.*, **104**, 43 (1979).
27. A. D. Schmidt and W. H. Ray, *Chem. Eng. Sci.*, **36**, 1401 (1981).
28. T. J. Tulig and M. Tirrell, *Macromolecules*, **14**, 1501 (1981).
29. W. Y. Chiu, G. M. Carratt and D. S. Soong, *Macromolecules*, **16**(3), 348 (1983).
30. Y. J. Huang and L. J. Lee, *AIChE J.*, **31**, 1585 (1985).
31. A. G. Mikos, C. G. Takoudis, and N. A. Peppas, *Macromolecules*, **19**, 2174 (1986).
32. L. T. Biegler, *Comput. Chem. Eng.*, **8**(314), 243 (1984).
33. J. E. Cuthrell and L. T. Biegler, *AIChE J.*, **33**, 1257 (1987).
34. R. G. Gottlieb, *AIAA J.*, **5**(2), 322 (1967).

35. A. E. Bryson and W. F. Denham, *J. Appl. Mech.*, **29**, 247 (1962).
36. M. M. Denn, *Optimization by Variational Methods*, reprint, Kreiger, Huntington, NY, 1978.
37. Y. J. Huang, J. D. Fan, and L. J. Lee, *J. Appl. Polym. Sci.*, **33**, 1315 (1987).
38. G. Z. A. Wu, M.S. thesis, University of Massachusetts, 1978.
39. A. W. Hui and A. E. Hamielec, *J. Appl. Polym. Sci.*, **16**, 749 (1972).
40. F. L. Marten and A. E. Hamielec, *J. Appl. Polym. Sci.*, **27**, 489 (1982).
41. J. Brandrup and E. H. Immergut, *Polymer Handbook*, 2nd ed., Wiley, New York, 1975.
42. Y. J. Huang, M.S. thesis, The Ohio State Univeristy, 1983.

Received April 6, 1989

Accepted July 13, 1989